Journal of Modern Applied Statistical Methods

Volume 15 | Issue 1 Article 40

5-1-2016

Analysis and Modeling of Statistical Properties of FMDFB Subband Coefficients

E. Jebamalar Leavline
Anna University, Tiruchirappalli, India, jebi.lee@gmail.com

Sutha Shunmugam
University College of Engineering, Panruti, suthapadmanabhan@gmail.com

DOI: 10.22237/jmasm/1462077540

Journal of Modern Applied Statistical Methods
May 2016, Vol. 15, No. 1, 802-824.

ISSN 1538 − 9472

Analysis and Modeling of Statistical Properties of FMDFB Subband Coefficients

E. Jebamalar Leavline
Anna University
Tiruchirappalli, India

Shunmugam Sutha
University College of Engineering
Panruti, India

Fast Multiscale Directional Filter Bank (FMDFB) is an image representation scheme used in several image processing applications. The statistical nature of the FMDFB subbands is analyzed, and a mathematical model of FMDFB coefficients is proposed. Experimental results are justified by goodness-of-fit tests.

Keywords: Statistical analysis, FMDFB, Subbands, Mathematical modeling, Gaussian distribution

Introduction

Statistical analysis plays a vital role in image processing and analysis. In high level image processing such as feature extraction, image analysis, segmentation and object recognition, extraction of statistical features is an important step and these statistical features are used along with the shape features to train the classifier. In other low level image processing methods such as image enhancement and restoration, the statistical analysis is useful to determine the parameters required to perform enhancement and restoration (Hyvärinen, Hurri, & Hoyer, 2009).

The use of multiscale transforms in digital image processing is widely addressed in image processing literature. Fast multiscale directional filter bank is an image representation scheme that is successfully used in feature extraction and image enhancement (Cheng, Law, & Siu, 2007a), (Cheng, Law, & Siu, 2007b). In our previous work, an image denoising scheme with FMDFB is proposed that works well for additive Gaussian and multiplicative speckle noise removal compared to other conventional multiscale denoising methods such as wavelet

Dr. E. Jebamalar Leavline is an Assistant Professor in the Department of Electronics and Communication Engineering. Email her at: jebi.lee@gmail.com. Dr. Sutha is an Assistant Professor in the Department of Electrical and Electronics Engineering. Email her at: suthapadmanabhan@gmail.com.

and contourlet based denoising (Leavline, Sutha, & Singh, 2014a). Yet, the statistical nature of the FMDFB subbands has not been analyzed.

Fast Multiscale Direction Filter Banks (FMDFB)

The major drawback of wavelet transform is that it is not being capable of capturing directional information effectively (Po & Do, 2006). This drawback is overcome by employing multiscale and directional representations that capture the geometrical structures in images such as smooth contours (Leavline, Sutha, & Singh, 2014b), (Do & Vetterli, 2005). In spite of high computation complexity and overcompleteness, the multiscale transforms are preferred in various applications because of their ability to represent fine details of the natural images. Pyramidal directional filter banks (PDFB) is one such multiscale image representation scheme, also termed as contourlet. A modification to the PDFB was proposed, namely the multiscale directional filter bank (MDFB) that is redundant in nature and a number of possible structures are available based on the choice of lowpass filter and the number of directional decomposition. According to Cheng et al (2007a), MDFB introduces an additional decomposition in the high-frequency band and thereby improves the radial frequency resolution at a cost of one set of extra scale and directional decompositions on the full image size. This results in increased number of computations. Also, MDFB has a higher redundancy than PDFB. The over completeness and increased frequency resolution of MDFB was found useful in applications like texture characterization and retrieval (Cheng et al., 2007a).

Cheng et al. (2007b) proposed a fast and reduced redundancy structure for this MDFB (FMDFB). This structure has the same redundancy as PDFB and 33% reduction in computational complexity compared to MDFB. Also, FMDFB exhibits perfect reconstruction irrespective of the choice of low pass filters. The total number of FMDFB directional subband coefficients is the same as the size of the original image because of the critically sampled DFB, and hence no extra computations are introduced by the scale decomposition. The computational complexity of FMDFB (Cheng et al., 2007b) is approximated as

$$\left(\frac{19}{3}+\frac{8}{3}L_d\right)MN \tag{1}$$

FMDFB outperforms MDFB in texture retrieval. In our previous work, we have introduced a multiscale denoising approach using FMDFB for Gaussian and speckle noise removal (Leavline et al., 2014a; Leavline & Sutha, 2011).

Statistical Analysis of FMDFB Subbands

Need for Statistical Analysis:

Statistical analysis plays a vital role in all areas of image processing. Although the usefulness of FMDFB has been demonstrated in image processing, it has not been extensively studied. Hence, analysis of statistical nature of the FMDFB subbands and a generalized mathematical model of FMDFB subbands is essential to aid the use of FMDFB in various applications.

Statistical measures

Several statistical measures used to analyze the statistical nature of the FMDFB subbands are presented.

Mean: It is the most common statistical measure as in Equation (2). It gives the average value of intensity level of the image.

$$\mu_x = \frac{1}{MN}\sum_{i=1}^{M}\sum_{j=1}^{N} x(i,j) \tag{2}$$

where μ_x is the mean value of the image $x(i, j)$ of size $M \times N$.

Median: It is a measure of much importance as it has a breakdown point of 50%. It represents the mid intensity value present in an image.

Mode: Mode is the most frequently occurring intensity value in $x(i, j)$ of size $M \times N$. However, the mode is not suitable for finding peaks in distributions having multiple modes.

Standard deviation: It is the measure of how the image intensity is spread from its average intensity μ_x. It is calculated as the square root of variance and given as

$$\sigma_x = \sqrt{\frac{1}{MN}\sum_{i=1}^{M}\sum_{j=1}^{N}\left[x(i,j)-\mu_x\right]^2} \tag{3}$$

Variance: It is the average of squared difference between $x(i, j)$ and μ_x calculated as square of standard deviation.

$$Var_x = \frac{1}{MN}\sum_{i=1}^{M}\sum_{j=1}^{N}\left[x(i,j)-\mu_x\right]^2 \tag{4}$$

Geometric mean: The geometric mean is less than or equal to the arithmetic mean unless all the intensity levels equal. It expresses the central tendency of the intensity values using the product of their values. The geometric mean is generally defined as the n^{th} root of the product of 'n' numbers.

$$GM_x = \left[\prod_{i,j=1}^{M,N} x(i,j)\right]^{1/MN} \tag{5}$$

Harmonic mean: Harmonic mean is calculated as the reciprocal of the arithmetic mean of the reciprocals. It is less than or equal to arithmetic mean. It is also called as sub-contrary mean.

$$HM_x = \frac{MN}{\sum_{i,j=1}^{M,N}\frac{1}{x(i,j)}} \tag{6}$$

Trimmed-mean: The trimmed-mean is a robust estimate of the location of a pixel $x(i, j)$. It calculates the mean by excluding 'K' smallest and largest intensity values. It is a representative estimate of the central intensity values of the image in the presence of outlier intensities. If $t(k, l)$ represents the trimmed intensity values with $k = 1, 2,\ldots,K$ and $l = 1, 2,\ldots,L$ the trimmed-mean is calculated as

$$TM_x = \frac{\sum_{k,l=1}^{K,L} t(k,l)}{KL} \tag{7}$$

Range: Range is the difference between minimum and maximum intensity level present in the image.

$$Range_x = \max\left(x(i,j)\right) - \min\left(x(i,j)\right) \tag{8}$$

Inter-quartile range: It is also known as midspread and is calculated as the difference between the 75th and the 25th percentiles of the intensity values of the image.

Mean absolute deviation: It is also termed as mean deviation or average absolute deviation. It is the mean of absolute deviation of a particular intensity level from the mean intensity level. This measure is computationally efficient than standard deviation.

$$MAD = \frac{1}{MN}\left[\left|x(i,j) - \mu_x\right|\right] \tag{9}$$

Gray Level Co-occurrence Matrix (GLCM): It is calculated as how often a pixel with gray-level (grayscale intensity) value '*g*' occurs horizontally adjacent to a pixel with the value '*h*'. Another name for a gray-level co-occurrence matrix is a gray-level spatial dependence matrix. The measures such as contrast, energy, homogeneity, entropy, and correlation are calculated from normalized GLCM.

Contrast: It is intensity contrast between a pixel and its neighbor over the whole image.

$$C_x = \sum_{g,h}\left|g-h\right|^2 GLCM\left(g,h\right) \tag{10}$$

Energy: It is the sum of squared elements in the GLCM.

$$E_x = \sum_{g,h}\left[GLCM\left(g,h\right)\right]^2 \tag{11}$$

Homogeneity: It is the measure of the closeness of the distribution of elements in the GLCM to the GLCM diagonal.

$$H_x = \sum_{g,h} \frac{GLCM(g,h)}{1+|g-h|} \tag{12}$$

Entropy: Entropy is a statistical measure of randomness that can be used to characterize the texture of the input image.

$$Entropy_x = -\sum p(x) \log_2 p(x) \tag{13}$$

Correlation: Correlation between two images $x(i, j)$ and $y(i, j)$ is calculated as

$$r = \frac{\sum_i \sum_j \left(x(i,j) - \mu_x\right)\left(y(i,j) - \mu_y\right)}{\sqrt{\left(\sum_i \sum_j x(i,j) - \mu_x\right)^2 \left(\sum_i \sum_j y(i,j) - \mu_y\right)^2}} \tag{14}$$

Moments: The central moment of order 'n' is defined as

$$m_n = E(x-\mu)^n \tag{15}$$

The central first moment is zero, and the second central moment is the variance. The third and fourth central moments are used to find the skewness and kurtosis. The normalized n^{th} central moment is calculated as the n^{th} central moment divided by σ^n.

Mathematical Modeling of FMDFB coefficients

A statistical model for FMDFB transform coefficients will now be developed. A computationally efficient and accurate model of FMDFB coefficients is necessary to assist straightforward parameter estimation needed for various image processing applications (Sutha, Leavline, & Gnana Singh, 2013). First, to find a suitable statistical model (Kwitt, 2010), the frequency distribution of FMDFB subbands need to be analyzed. For this purpose, we use the classical histogram. Also, the histogram is plotted along with the Gaussian fit function that is shown red in color in Figure 1 to Figure 4.

The goodness-of-fit (GoF) of the FMDFB subband coefficients with the Gaussian distribution is evaluated with the help of Quantile–Quantile plot (Q-Q

plot) as a graphical tool. The Q-Q plots of FMDFB subbands of a clean image shows that, except the tail regions at both the ends, the FMDFB subbands coincide with the Gaussian (normal) distribution shown red in color in Figure 5 and 6. However, it is evident from the Q-Q plots of the FMDFB subbands of noisy image that they overlap with the Gaussian (normal) distribution at most of the points as in Figure 7 and 8.

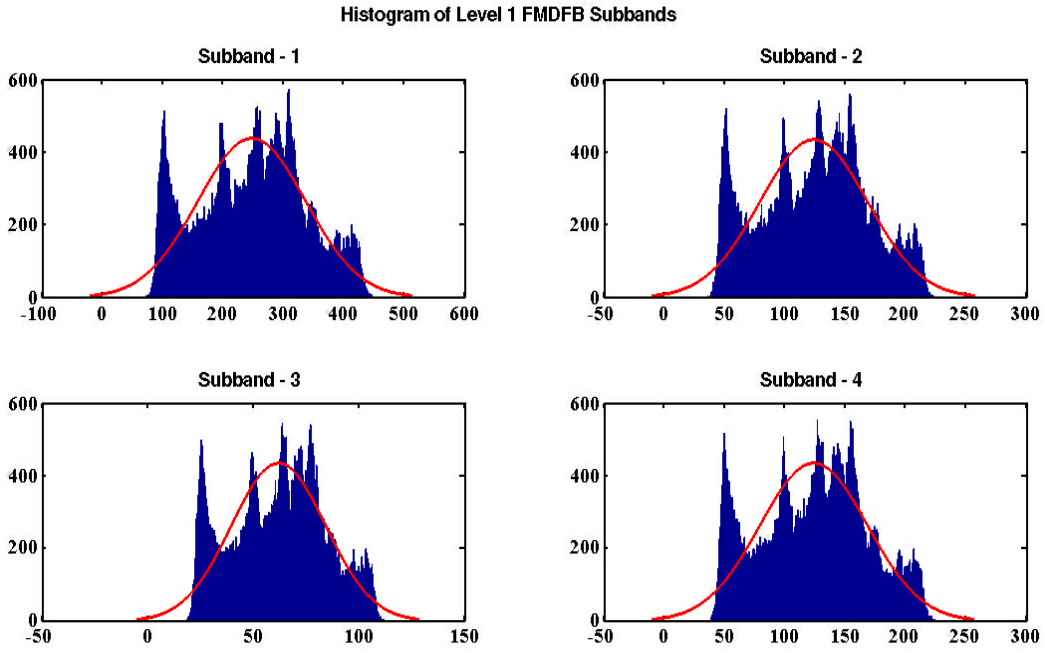

Figure 1. Histogram of level 1 FMDFB subbands of clean Lena image

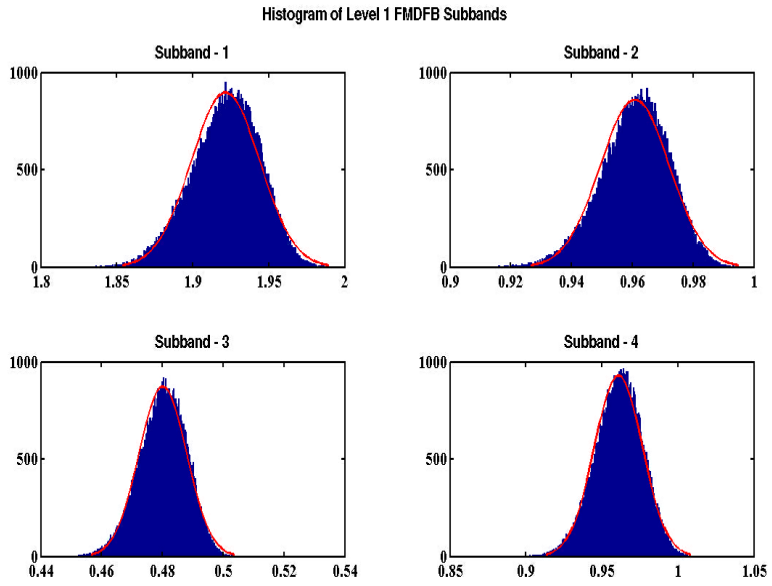

Figure 2. Histogram of level 1 FMDFB subbands of Lena image with AWGN with variance 0.001

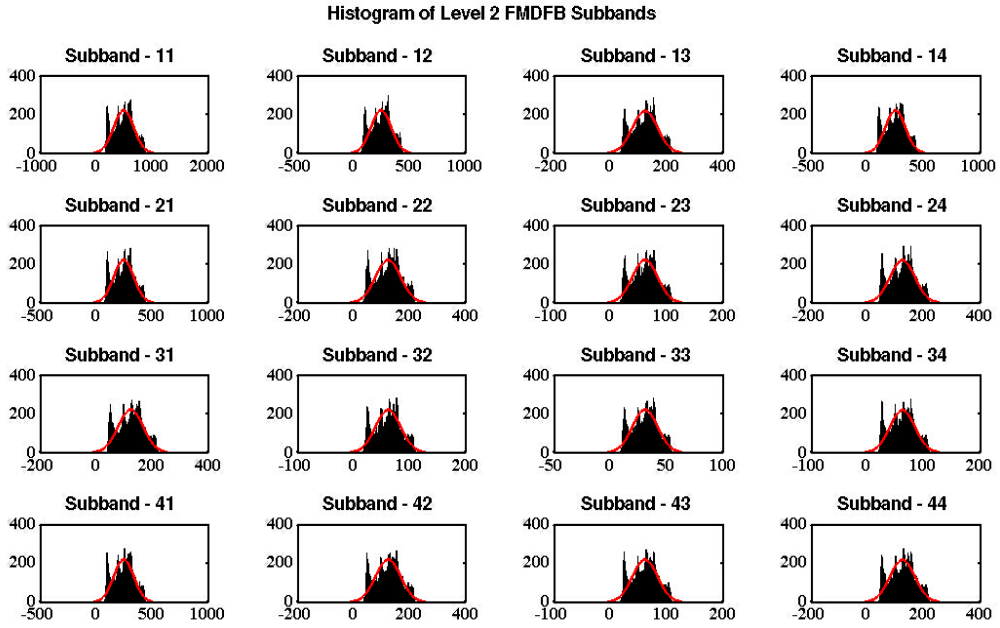

Figure 3. Histogram of level 2 FMDFB subbands of clean Lena image

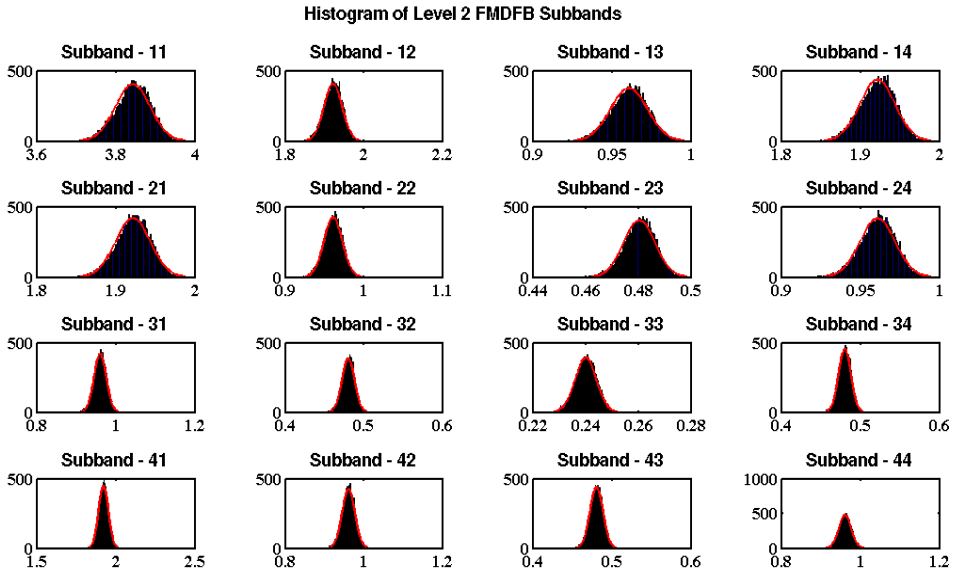

Figure 4. Histogram of level 2 FMDFB subbands of Lena image with AWGN with variance 0.001

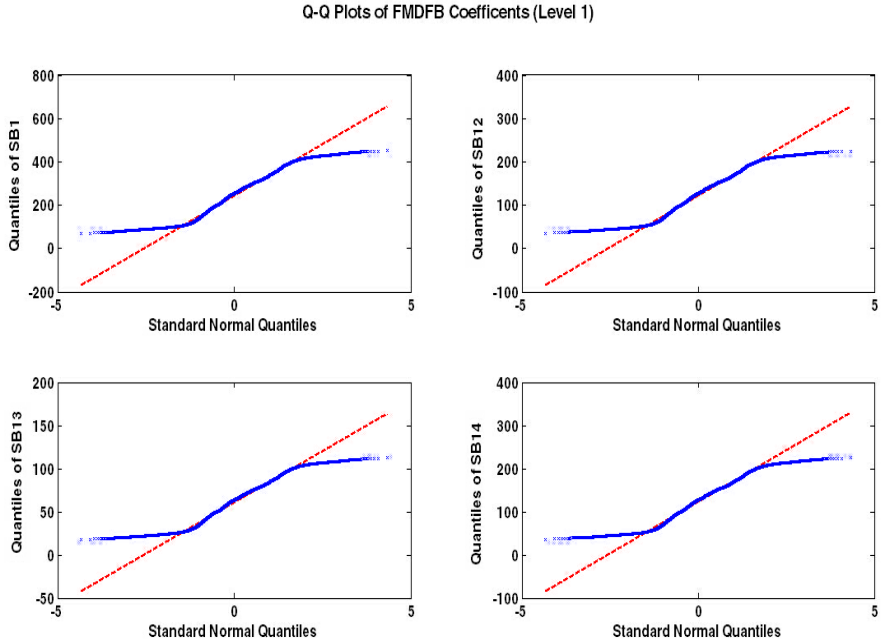

Figure 5. Quantile – Quantile plot of level 1 FMDFB subband coefficients of clean Lena image

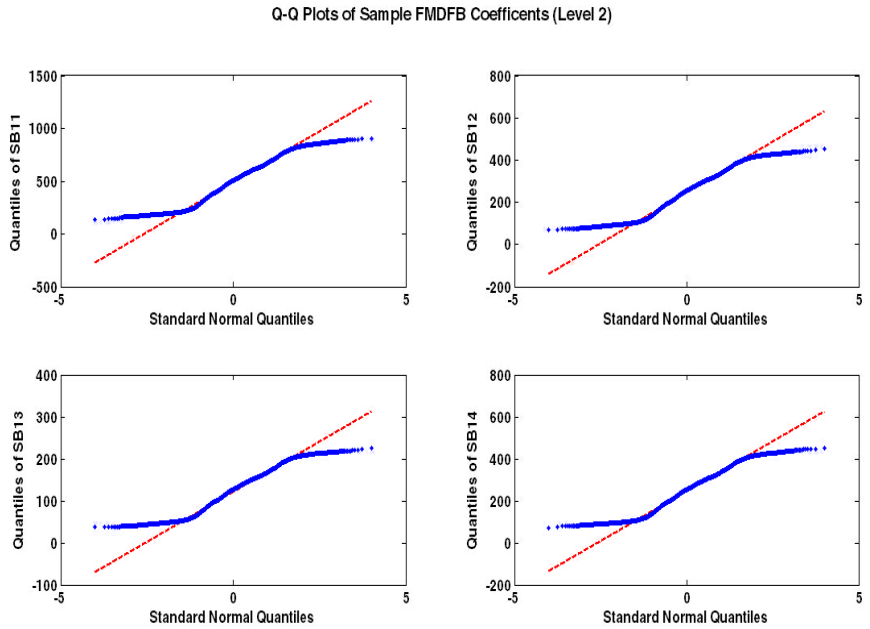

Figure 6. Quantile – Quantile plot of sample level 2 FMDFB subband coefficients of clean Lena image

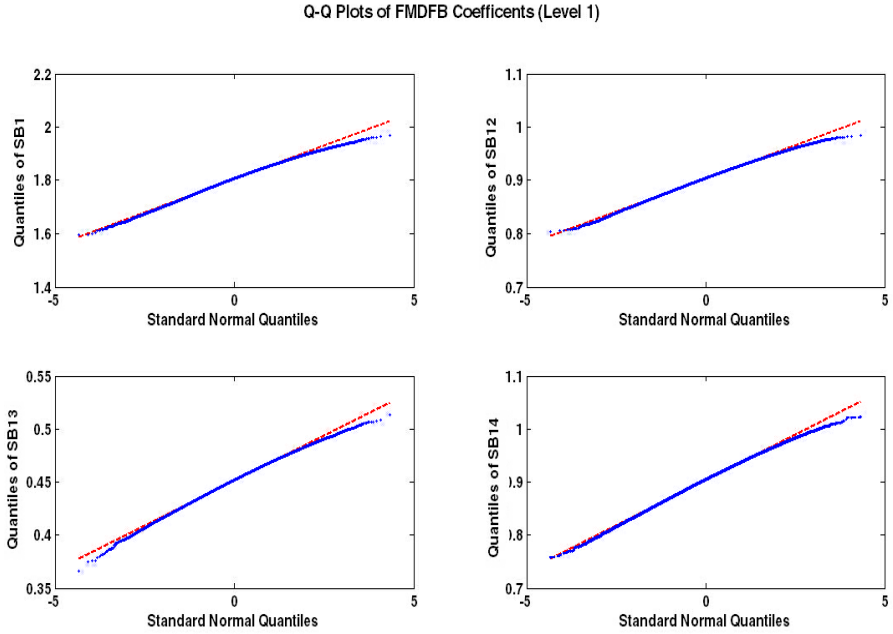

Figure 7. Quantile – Quantile plot of level 1 FMDFB subband coefficients of Lena image with AWGN with variance 0.001

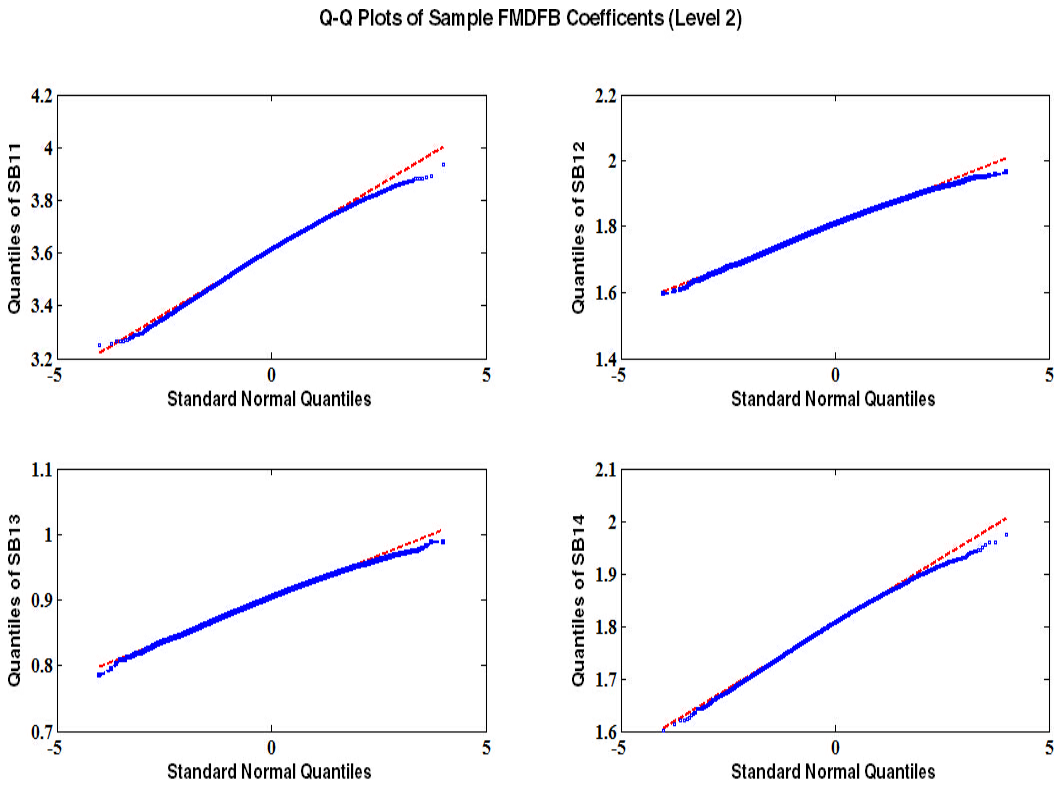

Figure 8. Quantile–Quantile plot of sample level 2 FMDFB subband coefficients of Lena image with AWGN with variance 0.001

To add strength to this argument, the GoF is tested using the Chi-Squared test. The MATLAB ("MATLAB") statistical toolbox function [*h*, *p*, *stat*] = *chi2gof*(*x*) is used that performs a chi-square goodness-of-fit test of the default null hypothesis that the data in vector '*x*' are a random sample from a normal distribution with mean and variance estimated from '*x*', against the alternative that the data are not normally distributed with the estimated mean and variance. The result '*h*' is 1 if the null hypothesis can be rejected at the 5% significance level denoted as 'α'. The result '*h*' is 0 if the null hypothesis cannot be rejected at the 5% significance level. The '*p*' value is the probability, under assumption of the null hypothesis of observing the given statistic and '*stat*' is the chi-squared statistics. The following procedure is followed to perform the chi-square goodness-of-fit test.

Step 1. The image is read and decomposed using FMDFB into subbands. In this experiment, the scale (*s*) and directional (*l*) decomposition

is fixed as 2. For this specification, there will be four and sixteen subbands at level 1 and level 2 of decomposition respectively. We denote the level 1 subband as $SB_{i,j}$, $i = 1,2 \ldots 2^s$, $j = 0$ and level 2 subbands as SB_{ij}, $i = 1,2 \ldots 2^s$, $j = 1,2,.., 2^l$

Step 2. For a subband SB_{ij}, the parameters of Gaussian (normal) distribution mean (μ) and standard deviation (σ) are estimated using maximum likelihood estimator with 95% confidence interval.

Step 3. Using the estimated 'μ' and 'σ', a reference Gaussian (normal) distribution is generated. From this distribution, 'N' samples are selected uniformly at random without replacement.

Step 4. Then the chi-square goodness-of-fit is calculated. If the '*Chi*2*Stat*' is less than the critical value calculated from the chi square table for the particular degrees of freedom the null hypothesis is accepted and it is rejected otherwise following the test hypothesis given below.

H_0. The coefficients of FMDFB subbands are consistent with the Gaussian (normal) distribution.

H_a. The coefficients of FMDFB subbands are not consistent with the Gaussian (normal) distribution.

The *h*, *p* and *stat* of the FMDFB subbands are indicted in Table 1. '*h*' represents whether the null hypothesis is accepted or rejected. '*p*' represents the probability with which the test hypothesis is accepted. If '*p*' is less than 0.05, then the null hypothesis is rejected. The parameter '*stat*' contains the chi square test value and the degrees of freedom. It is evident from Table 1 that the null hypothesis is rejected only for a few subbands. Further, the above mentioned test is also conducted on various standard gray scale images. The average rate of hypothesis acceptance is 96.66% as shown in Table 2. Hence, the Gaussian probability distribution assumption of FMDFB subbands holds good.

Table 1. Results of Chi-square test of FMDFB subbands

Subbands	Clean Lena Image				Noisy Lena Image with AWGN 0.001				Noisy Lena Image with Speckle 0.04			
	h	*p*	*Chi*2 value	DoF	*h*	*p*	*Chi*2 value	DoF	*h*	*p*	*Chi*2 value	DoF
SB10	0	0.0619	8.966	4	0	0.6666	4.0746	6	0	0.7094	3.7582	6
SB20	0	0.8250	3.595	7	0	0.6189	4.4283	6	1	0.0106	16.663	6
SB30	0	0.0629	13.403	7	0	0.3055	8.3162	7	0	0.4252	7.0357	7
SB40	0	0.9880	0.934	6	0	0.2133	7.0999	5	0	0.3602	5.4796	5
SB11	0	0.8685	3.174	7	0	0.5592	3.9322	5	0	0.7147	2.9049	5
SB12	0	0.4215	6.014	6	0	0.8168	2.9363	6	0	0.4700	5.5950	6
SB13	0	0.4504	5.762	6	1	0.0219	13.1671	5	0	0.8535	3.3245	7
SB14	0	0.6165	4.446	6	0	0.3267	5.7949	5	0	0.1704	7.7525	5
SB21	0	0.2525	9.002	7	1	0.0170	13.7923	5	0	0.5547	4.9158	6
SB22	0	0.0883	12.394	7	0	0.7317	2.7943	5	0	0.9317	2.4384	7
SB23	0	0.4344	5.900	6	0	0.7267	2.0492	4	0	0.7336	3.5775	6
SB24	0	0.8166	3.672	7	1	0.0202	15.0073	6	0	0.2490	9.0512	7
SB31	0	0.7600	3.379	6	0	0.2208	6.9979	5	0	0.6080	4.5101	6
SB32	1	0.0339	13.644	6	0	0.2470	9.0794	7	0	0.5819	4.7068	6
SB33	0	0.3148	7.065	6	0	0.9336	2.4122	7	0	0.3610	6.5839	6
SB34	1	0.0144	17.504	7	0	0.3168	5.8930	5	0	0.4185	7.1002	7
SB41	0	0.4566	5.708	6	0	0.2594	8.9073	7	0	0.2283	8.1362	6
SB42	0	0.4582	5.695	6	0	0.4941	6.3979	7	0	0.5778	5.6780	7
SB43	0	0.7084	3.765	6	0	0.6206	5.3228	7	0	0.1495	8.1237	5
SB44	0	0.0870	11.045	6	0	0.4728	5.5716	6	0	0.8157	2.9453	6

Table 2. Summary of chi-square goodness of fit test for 20 gray scale images

Image	Clean Image		Image with Gaussian Noise (zero mean & 0.001 variance)		Image with Speckle Noise (0.04 variance)	
	Accepted Subbands	Rejected Subbands	Accepted Subbands	Rejected Subbands	Accepted Subbands	Rejected Subbands
Total	385	15	390	10	385	15
Acceptance (%)	96.25		97.5		96.25	

FMDFB Subband Model:

FMDFB is an orthogonal filter bank structure that is critically sampled in nature. It is a multiresolution and directional scheme that is useful for image representation. In order to visualize the nature of the FMDFB subband coefficients, the histogram fit and chi-square goodness-of-fit test are performed. From the discussions presented in the previous section, it is concluded that the FMDFB subbands follow the Gaussian (Normal) distribution with mean 'μ' and standard deviation 'σ'. Following that, the FMDFB coefficients are mathematically modeled with the following assumptions.

Assumption 1. The coefficients of any FMDFB subband are identically distributed with the same probability density function.

Assumption 2. The coefficients of FMDFB subbands of the same level of decomposition are not independent and they are highly correlated.

Assumption 3. The coefficients of FMDFB subbands of different levels of decomposition are independent and they are not correlated.

With a scale decomposition of 's', and level of directional decomposition 'l', the FMDFB subband coefficients are represented as in Equation (16) where 'γ' is the FMDFB subband.

$$\psi^{(l,s)} = \begin{cases} \{\gamma_i\}, i = 1, 2, \ldots 2^l, \text{ for } s = 1 \\ \{\gamma_{ij}\}, i - 1, 2, \ldots 2^l, j = 1, 2, \ldots, 2^s \text{ for } s \neq 1 \end{cases} \tag{16}$$

The standard Gaussian (normal) distribution of a random function 'g' follows the probability density function given by Equation (17) with mean μ = 0 and variance σ = 1.

$$f\left(g,\mu,\sigma\right)=\frac{1}{\sqrt{2\Pi}}e^{-\frac{g^2}{2}} \tag{17}$$

Then the probability density function $\zeta(.)$ of the FMDFB coefficients is modeled as in Equation (18). Here, γ_{ij} are the coefficients of FMDFB subband, μ_γ and σ_γ are the mean and standard deviation of the FMDFB subband under consideration.

$$\zeta\left(\gamma_{ij},\mu_\gamma,\sigma_\gamma\right)=\frac{1}{\sigma_\gamma\sqrt{2\Pi}}e^{-\frac{\left(\gamma_{ij}-\mu_\gamma\right)^2}{2\sigma_\gamma^2}} \tag{18}$$

Results and Discussion

Experimental Setup:

The analysis of statistical characteristics of FMDFB subbands is carried out in MATLAB environment on standard test images. The statistical measures are calculated on images with the help of MATLAB Statistics Toolbox and Image Processing Toolbox.

Results and Discussion:

The statistical measures are calculated on clean image and noisy image. The comparison of various statistical measures is shown in Table 3 for various noise densities. Also, the noisy image is decomposed using FMDFB with scale and directional decomposition levels set to 2. This will result in 16 subbands. Further, the statistical measures of all the sixteen FMDFB directional subband coefficients are calculated and tabulated in Table 4. Correlation between pairs of subbands is studied at level 1 and level 2 of FMDFB decomposition as shown in Table 5 and Table 6. An analysis of first, second and higher order moments is carried out and the moments for level 1 and level 2 FMDFB subbands are shown in Figure 9. The histograms of level 1 and level 2 FMDFB subbands of clean and noisy image with speckle noise are shown in Figure 10 and Figure 11.

The following facts are inferred from the experimental results.

(i) The mean, standard deviation and mean absolute deviation (MAD) of the image vary linearly with the level of noise present.

(ii) The geometric mean and harmonic mean are non zero for clean image and they become zero for noisy image. However, at some higher noise levels, these two statistical parameters become non zero.

(iii) Energy and homogeneity of the intensity values are almost constant and equal to 1. But entropy is non zero and is not constant with respect to the level of noise present.

(iv) After performing FMDFB decomposition, the subband SB11 exhibits maximum magnitudes for all statistical measures compared at a particular noise level. On the other hand the subband SB33 exhibits maximum magnitudes for all statistical measures compared.

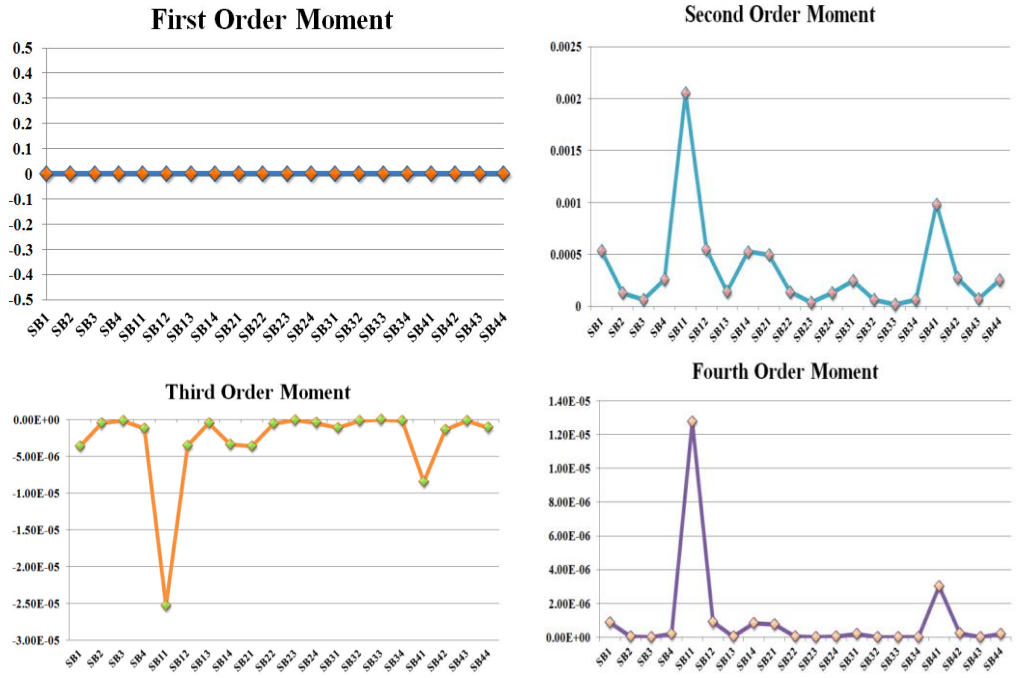

Figure 9. First, Second and higher order moments of FMDFB Subbands

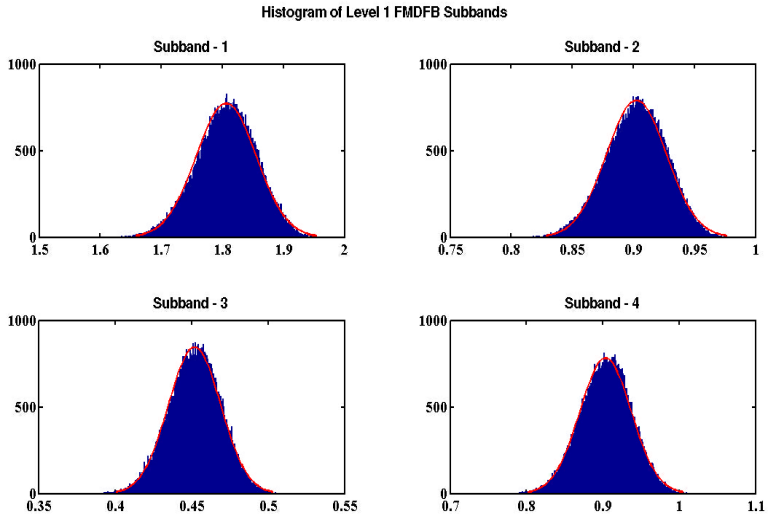

Figure 10. Histogram of level 1 FMDFB subbands of Lena image with speckle noise with variance 0.04

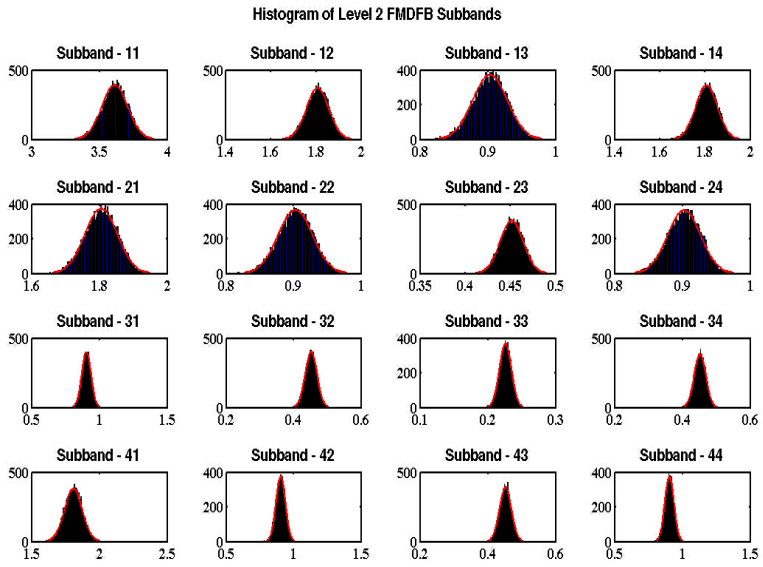

Figure 11. Histogram of level 2 FMDFB subbands of Lena image with speckle noise with variance 0.04

(v) However, the energy and homogeneity are constant and equal to 1 for all subbands irrespective of the level of decomposition, and the entropy is maintained at zero. Energy is equal to 1 for clean images and the homogeneity of magnitude 1 represents that all the subbands are smooth in nature. Also, lower entropy values depict that the subbands are having smooth texture.

(vi) Among the level 1 subbands, {SB3, SB4} subband pair exhibits less correlation compared to other pairs of subbands. However, the correlation coefficients of all level 1 subbands are close to unity, showing higher degree of correlation.

(vii) In level 2, the subbands {SB11, SB33} subband pair exhibits less correlation.

(viii) From the analysis of lower and higher order central moments, it is observed that, all the subbands have the first order central moment as zero. This shows that all the FMDFB subbands follow a distribution with zero mean. The second moment is the variance of each subband and SB11 has maximum variance meaning that the coefficients of SB11 subband are spread over a wide range.

(ix) The third normalized central moment is a measure of skewness of the histogram. The coefficients of all FMDFB subbands have negative skewness. This means that the histograms of the subbands are skewed towards the left. However, since the skewness is near zero, the distribution of the subband coefficients can be characterized as near symmetric. The fourth normalized central moment is a measure of shape of the distribution. The kurtosis values of all the subbands are above zero (positive). This ensures that there will be a peak in the distribution which falls at the mean. The average magnitude of excess kurtosis of subbands is near zero. Hence the shape of the distribution can be characterized as Gaussian (Normal). Also, the average proper kurtosis of FMDFB subbands of a noisy image is approximately 3 leading to Gaussian (Normal) distribution. However, the average proper kurtosis of FMDFB subbands of a clean image is less than 3 leading to sub-Gaussian (sub-Normal) distribution or Platykurtic distribution.

(x) The images corrupted with Gaussian noise and speckle noise follow similar probability distribution as in Figure 10 and Figure 11.

Table 3. Comparison of various statistical measures of clean and noisy images

Gaussian Noise Variance	Mean	Median	Mode	SD	Variance	GM	HM	TM	IQR	MAD	Range	Contrast	Corre-lation	Energy	Homo-geneity	Entropy
Clean Image	123.61	140	99	12.531	822850	112.52	99.84	124.11	35	9.418	193	0	-	1	1	0
0.001	123.94	133	0	9.667	812257.4	0	0	124.37	27.25	7.221	117	0.530	0.036	0.978	0.991	0.050
0.005	124.85	134	0	9.695	808297.7	0	0	125.29	27.25	7.232	115	0.475	0.029	0.980	0.992	0.046
0.01	126.10	136	0	9.732	819356	0	0	126.60	27	7.256	125	0.436	0.030	0.982	0.992	0.042
0.02	128.68	138.25	255	9.576	794593.6	0	0	129.15	27.5	7.148	112	0.355	0.023	0.985	0.994	0.035
0.03	131.12	140.25	255	9.670	809828.5	0	0	131.69	28	7.200	118	0.272	0.021	0.989	0.995	0.028
0.04	133.76	143	255	9.631	798620.9	0	0	134.32	28	7.244	114	0.223	0.024	0.991	0.996	0.024
0.05	136.24	145.75	255	9.645	804415.7	0	0	136.86	27.5	7.208	119	0.178	0.017	0.993	0.997	0.020
0.06	138.79	148.5	255	9.625	801055.4	0	0	139.37	27.5	7.197	119	0.139	0.009	0.994	0.998	0.016
0.07	141.25	150.25	255	9.611	789655	0	0	141.80	27	7.204	124	0.099	-0.001	0.996	0.998	0.012
0.08	143.79	153	255	9.522	773594.8	0	0	144.49	28.75	7.203	122	0.075	0.009	0.997	0.999	0.009
0.09	146.32	155.75	255	9.511	769365.9	0	0	146.94	29	7.200	126	0.052	0.007	0.998	0.999	0.007
0.1	148.85	158.25	255	9.496	767611.6	0	0	149.60	27.5	7.129	134	0.040	0.000	0.998	0.999	0.005
0.2	173.32	184.75	255	9.009	620831.8	0	0	175.15	28.5	6.958	156	0.002	0.000	1.000	1.000	0.000

Table 4. Comparison of various statistical measures of different FMDFB subbands (level 1 and level 2)

FMDFB Subbands	Mean	Median	Mode	Standard Deviation	GM	HM	TM	IQR	MAD	Range
SB1	247.5	277.3	54.2	24.8	229.1	208.7	248.6	69.4	18.5	323.4
SB2	124.0	138.2	30.7	12.4	114.8	104.5	124.6	36.0	9.3	160.7
SB3	62.0	69.1	12.6	6.0	57.4	52.1	62.2	17.4	4.5	82.0
SB4	123.8	137.6	28.4	12.2	114.4	104.1	124.2	35.0	9.1	163.7
SB11	495.1	556.7	100.8	50.0	458.3	417.4	497.1	137.3	37.0	640.8
SB12	247.5	277.4	61.8	25.0	228.8	207.9	248.6	69.1	18.7	324.6
SB13	123.8	138.7	30.8	12.4	114.6	104.3	124.3	33.9	9.3	160.4
SB14	247.5	276.8	55.5	24.8	229.5	209.5	248.6	70.0	18.3	317.7
SB21	248.0	276.5	61.8	25.0	229.6	209.2	249.1	72.1	18.7	311.3
SB22	124.0	138.1	27.8	12.5	114.6	104.0	124.6	36.4	9.4	163.8
SB23	62.0	69.2	14.4	6.2	57.4	52.2	62.3	18.0	4.7	80.1
SB24	124.0	139.0	32.9	12.4	115.0	105.0	124.6	36.8	9.3	158.6
SB31	124.0	138.2	25.0	12.1	114.7	104.4	124.4	35.4	9.1	170.0
SB32	62.0	69.1	12.4	6.1	57.2	51.9	62.2	18.1	4.6	82.3
SB33	31.0	34.3	6.2	3.0	28.7	26.0	31.1	9.0	2.3	40.2
SB34	62.0	68.7	12.0	6.0	57.4	52.4	62.2	17.6	4.5	79.9
SB41	247.5	275.5	58.1	24.6	228.9	208.2	248.5	71.1	18.2	320.6
SB42	123.8	137.2	26.1	12.3	114.3	103.7	124.3	35.8	9.2	153.7
SB43	61.9	68.5	13.4	6.1	57.2	52.0	62.1	16.9	4.6	78.2
SB44	123.8	137.4	26.5	12.2	114.6	104.5	124.3	34.6	9.0	164.1

Table 5. Comparison of correlation between FMDFB subbands at level 1 (clean image)

Level 1 Subbands	SB1	SB2	SB3	SB4
SB1	1.00	0.98	0.97	0.98
SB2	0.98	1.00	0.98	0.98
SB3	0.97	0.98	1.00	0.96
SB4	0.98	0.98	0.96	1.00

Table 6. Comparison of correlation between FMDFB subbands at level 2 (clean image)

Level 2 Subbands	SB11	SB12	SB13	SB14	SB21	SB22	SB23	SB24	SB31	SB32	SB33	SB34	SB41	SB42	SB43	SB44
SB11	1.00	0.97	0.94	0.99	0.99	0.93	0.90	0.97	0.97	0.91	0.88	0.95	0.98	0.95	0.92	0.97
SB12	0.97	1.00	0.99	0.98	0.98	0.98	0.96	0.98	0.98	0.97	0.94	0.97	0.96	0.98	0.96	0.96
SB13	0.94	0.99	1.00	0.97	0.97	0.99	0.98	0.98	0.97	0.98	0.96	0.98	0.94	0.98	0.98	0.96
SB14	0.99	0.98	0.97	1.00	0.99	0.95	0.93	0.98	0.98	0.93	0.91	0.97	0.98	0.96	0.95	0.98
SB21	0.99	0.98	0.97	0.99	1.00	0.96	0.94	0.99	0.98	0.94	0.92	0.97	0.98	0.97	0.95	0.97
SB22	0.93	0.98	0.99	0.95	0.96	1.00	0.99	0.98	0.96	0.98	0.96	0.96	0.93	0.98	0.97	0.94
SB23	0.90	0.96	0.98	0.93	0.94	0.99	1.00	0.97	0.94	0.98	0.98	0.96	0.91	0.96	0.98	0.93
SB24	0.97	0.98	0.98	0.99	0.99	0.98	0.97	1.00	0.98	0.96	0.94	0.98	0.97	0.98	0.97	0.98
SB31	0.97	0.98	0.97	0.98	0.98	0.96	0.94	0.98	1.00	0.96	0.94	0.99	0.96	0.96	0.95	0.96
SB32	0.91	0.97	0.98	0.93	0.94	0.98	0.98	0.96	0.96	1.00	0.99	0.98	0.91	0.96	0.96	0.93
SB33	0.88	0.94	0.96	0.91	0.91	0.96	0.98	0.94	0.94	0.99	1.00	0.96	0.89	0.94	0.96	0.91
SB34	0.95	0.97	0.98	0.97	0.97	0.96	0.96	0.98	0.99	0.98	0.96	1.00	0.95	0.96	0.96	0.96
SB41	0.98	0.96	0.94	0.98	0.98	0.93	0.91	0.97	0.96	0.91	0.89	0.95	1.00	0.96	0.94	0.99
SB42	0.945	0.979	0.978	0.960	0.967	0.976	0.965	0.975	0.962	0.959	0.942	0.963	0.964	1.000	0.988	0.977
SB43	0.919	0.963	0.977	0.943	0.945	0.972	0.976	0.965	0.945	0.963	0.960	0.959	0.937	0.988	1.000	0.964
SB44	0.968	0.962	0.960	0.980	0.972	0.941	0.931	0.978	0.963	0.925	0.909	0.961	0.990	0.977	0.965	1.000

Conclusion

Experimental results revealed the FMDFB directional subbands follow Gaussian (normal) probability distribution with mean 'μ' and standard deviation 'σ'. This statistical model will be very much useful to estimate necessary parameters for image processing applications such as threshold estimation in denoising and segmentation and feature extraction.

References

Cheng, K.-O., Law, N.-F., & Siu, W.-C. (2007a). Multiscale directional filter bank with applications to structured and random texture retrieval. *Pattern Recognition*, *40*(4), 1182-1194. doi:10.1016/j.patcog.2006.07.014

Cheng, K.-O., Law, N.-F., & Siu, W.-C. (2007b). A novel fast and reduced redundancy structure for multiscale directional filter banks. *IEEE Transactions on Image Processing*, *16*(8), 2058-2068. doi:10.1109/TIP.2007.901212

Do, M. N., & Vetterli, M. (2005). The contourlet transform: An efficient directional multiresolution image representation. *IEEE Transactions on Image Processing*, *14*(12), 2091-2106. doi:10.1109/TIP.2005.859376

Hyvärinen, A., Hurri, J., & Hoyer, P. O. (2009). *Natural image statistics: A probabilistic approach to early computational vision.* (Vol. 39). New York, NY: Springer. Retrieved May 27, 2014

Kwitt, R. (2010). *Statistical modeling in the wavelet domain and applications* (Doctoral thesis). University of Cambridge, Cambridge, United Kingdom. Retrieved May 27, 2014, from http://wavelab.at/papers/Kwitt10d.pdf

Leavline, E. J., & Sutha, S. (2011, June 3-5). Gaussian noise removal in gray scale images using fast multiscale directional filter banks. *Recent Trends in Information Technology (ICRTIT), 2011 International Conference on* (pp. 884-889). Presented at the 2011 International Conference on Recent Trends in Information Technology (ICRTIT), Chennai, India. doi:10.1109/ICRTIT.2011.5972377

Leavline, E. J., Sutha, S., & Singh, D. A. A. G. (2014a). Fast multiscale directional filter bank-based speckle mitigation in gallstone ultrasound images. *Journal of the Optical Society of America A*, *31*(2), 283-292. doi:10.1364/JOSAA.31.000283

Leavline, E. J., Sutha, S., & Singh, D. A. A. G. (2014b). On the suitability of multiscale image representation schemes as applied to noise removal. *International Journal of Innovative Computing, Information and Control*, *10*(3), 1135-1147.

MATLAB – The Language of Technical Computing – MathWorks India. Retrieved May 27, 2014, from http://www.mathworks.in/products/matlab/

Po, D. D.-Y., & Do, M. N. (2006). Directional multiscale modeling of images using the contourlet transform. *IEEE Transactions on Image Processing*, *15*(6), 1610-1620. doi:10.1109/TIP.2006.873450

Sutha, S., Leavline, E. J., & Gnana Singh, D. A. A. (2013). IHNS: A pragmatic investigation on identifying highly noisy subband in FMDFB for fixing threshold to deteriorate noise in images. *Information Technology Journal*, *12*(7), 1289-1298. doi:10.3923/itj.2013.1289.1298